Angewandte
Minireviews

Rare-Earth Metal Hydrides

DOI: 10.1002/anie.201108558

Oxidation by Hydrogen in the Chemistry and Physics of the Rare-Earth Metals**

*Arndt Simon**

amorphous materials · electron transport · hydrides · magnetic properties · rare earths

Rare-earth metals (RE) easily react with hydrogen. For decades the bonding of hydrogen has been discussed controversially in terms of either the "proton model" or the "anion model". Detailed investigations of metal-rich compounds of the rare-earth metals provide clear evidence for the incorporation of hydrogen as a hydride anion. Several categories of compounds can be distinguished regarding their behavior towards hydrogen. Low-valence compounds with metal–metal bonding frequently provide their excess electrons to form hydride ions as found with the halide hydrides $REXH_n$*. However, there are exceptions, such as, LaI which does not react with hydrogen as a result of special electronic and electrostatic conditions. The opposite is true with* La_2C_3 *although this compound does not provide excess metal valence electrons. An amorphous phase* $La_2C_3H_{1.5}$ *forms at very low temperature, around 450 K. The presence of hydrogen strongly influences the electrical and magnetic properties, for example, spin-glass formation and colossal magneto resistance arising in the presence of* $4f^n$ *cores with the lanthanoid elements.*

1. Intoduction

Rare-earth metals (*RE*) react with hydrogen even at room temperature. Eu and Yb form semiconducting dihydrides. EuH_2 and interestingly also ScH_2 are strictly stoichiometric, whereas Yb can absorb additional hydrogen and thus paves the way to the behavior of the trivalent *RE* metals. These form metallic dihydrides and incorporate further amounts of hydrogen up to the limiting composition of the insulating trihydrides. There is extensive literature on the *RE* hydrides comprehensively described in the Gmelin Handbook.[1] More recent work illuminated the complex phase relationships in *RE* hydrides and their structures and dynamics.[2,3] Innumerable publications cover the interaction of *RE* metals and hydrogen in multicomponent systems for possible applications which range from hydrogen storage to rechargeable batteries to switchable mirrors.

The metallic character of *RE* hydrides provoked intense and controversial discussions about chemical bonding which can be summarized in two alternative views. The "proton model" is based on the assumption that hydrogen donates its electron to the conduction band of d character and resides as a shielded proton in an alloy matrix. In contrast, the "anion model" postulates a reverse electron transfer from the metal to hydrogen resulting in the formation of hydride anions and, hence, predominantly ionic bonding. In chemical terms this controversy addresses the question as to whether hydrogen acts as a reducing agent, as usual, or as an oxidizing agent. The controversy can be clarified unequivocally by investigations of a broad range of *RE* metal compounds.

The important role of hydrogen in the chemistry of low-valence *RE* compounds was discovered by accident. In experiments aiming at the reduction of *RE* trihalides by their respective metals, phases of Y, Gd, and Tb were identified which had the crystal structures of Zr monohalides, Zr*X*.[4,5] However, it turned out that the yield of these new phases decreased with increased experience in preparation! Finally it became clear that they were actually stabilized by hydrogen, invisible to X-rays in the presence of strong scatterers, which was introduced by contamination of the metals and/or by traces of moisture. Heating these phases in sealed tantalum tubes under vacuum at the temperatures of their formation, the loss of hydrogen by diffusion through the container wall

---

[*] Prof. Dr. A. Simon
Max Planck Institute for Solid State Research
Heisenbergstrasse 1, 70569 Stuttgart (Germany)
E-mail: a.simon@fkf.mpg.de
Homepage: http://www.fkf.mpg.de/simon/

[**] The Minireview summarizes the contents of a talk the author gave when receiving the Terrae Rarae Award 2011.

led to a mixture of the educts,[6] and adding the appropriate amount of hydrogen on purpose resulted in high yields of $REX\mathrm{H}_n$. Once recognized, an interesting field of research opened.

In principle, the researchers should have been warned, because the first incorporation of hydrogen in a transition-metal compound, $\mathrm{Nb_6I_{11}H}$, had been discovered equally unexpectedly many years before.[7] This compound contains the M_6X_8-type cluster, and instead of a closed-shell configuration with 24 electrons in metal–metal bonding states for this type of cluster it has an electron deficiency with only 19 electrons per cluster available. This deficiency can be compensated by introducing an H atom, formally adding its electron to the M–M bonding system according to the "proton model". However, a closer look into the electronic band structure tells a different story.[8] One orbital of suitable symmetry mixes with the H1s state forming a bonding hydride-like state below and the antibonding combination above all the M–M bonding states. This bonding at the expense of M–M bonding is in agreement with the "anion model". In the case of the more electropositive character of the RE metals compared to Nb the H1s state enters at an even lower energy which leads to well defined hydride anions.

The behavior of hydrogen in the chemistry and physics of RE compounds is determined by two conditions, the electron count and the repulsive anion–anion interactions. There are three specific cases for the reaction of hydrogen to be discussed. 1) An excess of metal valence electrons in a low-valence compound provides the driving force for a reaction with hydrogen which localizes the electrons as hydride ions. 2) In spite of the presence of an excess of electrons no reaction with hydrogen occurs, and 3) surprisingly hydrogen enters the structure although there is no obvious excess of metal valence electrons present.

2. Hydrogen Localizes Excess Metal Valence Electrons

Moving from a discrete cluster to the infinite systems of condensed clusters does not change the arguments used above in describing the bonding of hydrogen. The structures of the halide carbides $RE_2X\mathrm{C}$ are composed of carbon-centered RE_6 octahedra condensed into layers (Figure 1). In an ionic description one metal valence electron per formula unit is used in extended M–M bonding according to $RE^{3+}{}_2X^-\mathrm{C}^{4-}\cdot\mathrm{e}^-$, and this electron can be "titrated" with hydrogen in a reversible topochemical reaction. Neutron diffraction experiments[9,10] performed on the deuterated Tb bromide compounds show that the D atoms slip into the centers of triangles in one metal-atom layer, push the C atoms towards the opposite layer of Tb atoms, which stays empty of hydrogen. The Br atoms move from the positions above faces to edges. All these atomic shifts reflect the repulsive interactions between the anions, D^-, Br^-, and C^{4-}. Of course, M–M bonding is lost as indicated by the change from low to high electrical resistance of the corresponding hydrogenated Gd compounds. There is one more interesting observation: The kink owing to ferromagnetic ordering in the metallic phase at 120 K vanishes in the non-conducting phase. In the insulating phase, magnetic order occurs only at liquid helium temperature. Clearly, the d conduction electrons provide magnetic coupling between the localized moments of the 4f electrons known as the RKKY interaction.

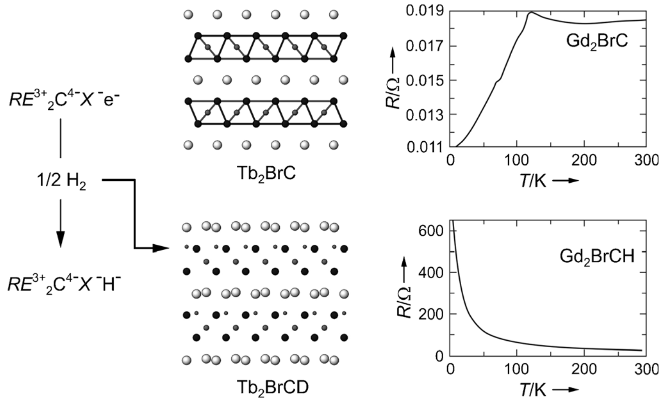

Figure 1. Reaction of hydrogen with phases $RE_2X\mathrm{C}$ (left), structural differences between $\mathrm{Tb_2BrC}$ and $\mathrm{Tb_2BrCD}$ (center), and change of the electrical properties measured for $\mathrm{Gd_2BrC}$ and $\mathrm{Gd_2BrCH}$ (right).

Arndt Simon, born 1940, became director at the Max Planck Institute of Solid State Research in 1974 and was in charge of his department until 2011.

The behavior of $SE_2X\mathrm{C}$ samples with intermediate H/D loadings was not investigated further, but this was done in great detail with the monohalide hydrides.[11] In their metallic phase the H atoms occupy a part of the tetrahedral voids up to full occupancy in $REX\mathrm{H}$. The halogen atoms X lie above the octahedral voids. The removal of more than 1/3 of the H atoms leads to decomposition into metal and trihalide which establishes the stability range for $REX\mathrm{H}_n$, $0.67 \le n \le 1.00$. In a reversible reaction hydrogen can be absorbed which enters the triangular faces of the octahedra (or rather trigonal antiprisms) resulting in a considerable increase of the distance between adjacent metal-atom layers, and the X atoms are shifted to positions above the tetrahedral voids. All these changes reflect the mutual repulsion between the anions in the salt like insulators $RE^{3+}X^-\mathrm{H}^-{}_2$. Whereas a range of homogeneity exists in $REX\mathrm{H}_n$ for $0.67 \le n \le 1.00$, a gap is found for $1.00 \le n \le 2.00$ which is due to the structural changes but also has an electronic reason essentially based on the avoidance of electron localization in Gd^{2+} ions. The antiferromagnetic ordering temperature is extremely sensitive to the hydrogen content which was determined both by volumetric measurements and combustion analyses. As demonstrated for GdBrH_n in Figure 2 marginal changes of the H content significantly influence the magnetic coupling.

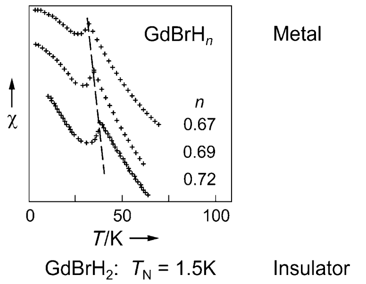

Figure 2. Antiferromagnetic ordering of metallic GdBrH$_n$ as a function of hydrogen content n in comparison with insulating GdBrH$_2$ which has a Neel temperature of 1.5 K.

Investigations on the isotypic Tb compounds allow a more quantitative understanding of the type of coupling. At nearly full occupancy of the tetrahedral voids, a Curie–Weiss law and a negative intercept with the abscissa is found, giving evidence for predominantly antiferromagnetic coupling. The decrease in hydrogen content shifts the intercept towards zero, and finally it becomes positive with ferromagnetic interactions dominating. The scenario is dominated by a competition between ferromagnetism and antiferromagnetism. Neutron diffraction experiments on TbBrD$_n$ show that for a value n near 1.00 the moments order ferromagnetically in each Tb atom layer, and adjacent layers arrange in an antiferromagnetic manner. With decreasing D content the magnetic superstructure reflections fade and finally vanish for lowest D content. So, long-range magnetic order is lost, however, short-range order still persists in the competition between ferro- and antiferromagnetism as indicated by a pronounced maximum in the magnetic susceptibility of TbBrD$_{0.7}$. To keep the story short, the competition between opposing magnetic interactions together with the disorder resulting from a partial occupation of voids by D atoms produces a spin glass. Interestingly, the disorder of the non-magnetic component D is the origin of spin-glass formation. Yet another intriguing phenomenon is observed with these monohalide hydrides: An external magnetic field changes their electrical conductivity dramatically, the colossal magneto-resistance (CMR) effect approaching 99.9% in a field of 7 Tesla at low temperatures.

A more detailed study of the magneto-resistance effect has been performed on the related but structurally simpler compound, GdI$_2$. It has the well-known crystal structure of NbSe$_2$ composed of close-packed single layers of metal atoms which are each coordinated by trigonal prisms of the nonmetal atoms. The preparation of GdI$_2$, in spite of its simplicity, provides a problem because the eutectic temperature for Gd/GdI$_3$ lies just 6 K below the peritectic decomposition of GdI$_2$.[12] Hence, to utilize the presence of some melt for enhancing the reaction rate the temperature has to remain within this limit. Obeying this precaution we were able to grow large single crystals at 1100 K which allows measurements of anisotropic properties.

In NbSe$_2$ the d electrons are involved in M–M bonding and play an important role in charge-density wave instability and superconductivity. Delocalized M–M bonding also occurs for GdI$_2$ according to the formulation $Gd^{3+}I^{-}_{2}\cdot e^{-}$, however, because of the presence of the magnetic 4f^7 core, superconductivity cannot occur. Instead, interesting magnetic properties come into focus. The magnetic moments couple through the d conduction electrons which lead to ferromagnetic order near room temperature. The ordering is accompanied by an anomaly in the electrical resistance which can be greatly influenced by an external magnetic field (Figure 3).[13]

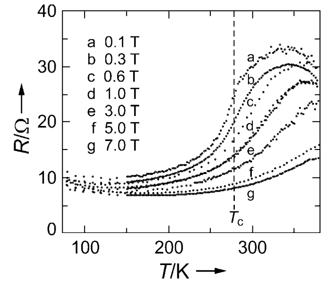

Figure 3. Colossal magneto resistance effect (CMR) of GdI$_2$ measured in magnetic fields between 0.1 and 7 Tesla.

The size of this CMR effect places GdI$_2$ in a large group of CMR materials which have been investigated and described in an enormous number of publications in recent years. Indeed, GdI$_2$ surpasses all of them at room temperature. In spite of the chemical differences, the origin of the effect is quite comparable in, for example, oxomanganates and GdI$_2$. In the oxomanganates the octahedral crystal field leads to a splitting of the d level into t_{2g} and e_g. Three electrons align with parallel spins in t_{2g}, and they order ferromagnetically, polarizing the conduction electrons in the e_g-type conduction band. Similarly, in the case of GdI$_2$, the 4f^7 cores order ferromagnetically and polarize the itinerant d band electrons. The electronic band structures of NbSe$_2$ and GdI$_2$ exhibit close similarities.[13] The Fermi surface of GdI$_2$ has tubular features along the z axis indicating the expected pronounced two-dimensional character, and it shows the nesting features of NbSe$_2$, however, slightly below the Fermi level. The idea lies at hand, to move into these singularities by lowering the Fermi level through hydrogen insertion, thus localizing some conduction electrons by hydride formation. The results of hydrogenation experiments were at first sight surprising, but finally they were quantitatively understood in terms of known principles.

The transition from GdI$_2$ to GdI$_2$H is completely homogeneous (Figure 4).[14] With the successive insertion of hydrogen the ferromagnetic saturation moment decreases steadily

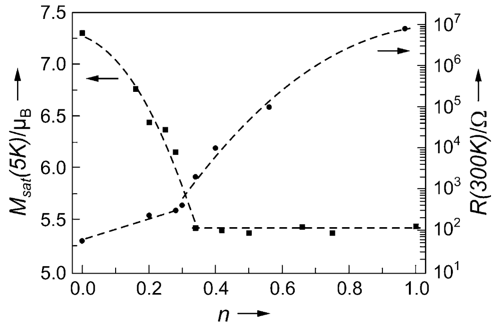

Figure 4. Changes of ferromagnetic saturation moment and electrical resistance of GdI$_2$H$_n$ as a function of hydrogen content n.

until it reaches a constant value at the approximate composition $GdI_2H_{0.33}$. The binding of conduction electrons as hydride anions is evident from the steep increase of the electrical resistance with hydrogen content. In the regime of still strong ferromagnetism at a chosen composition $GdI_2H_{0.2}$ colossal magneto resistance is observed (Figure 5). In the regime of constant saturation moment, above the composition $GdI_2H_{0.33}$, spin-glass behavior occurs as evidenced by the frequency dependences of the real part and characteristic absorption in the imaginary part of the magnetic susceptibility of a sample $GdI_2H_{0.42}$ (Figure 6). The phase diagram is thus characterized by different areas determined by paramagnetism, ferromagnetism, mixed ferromagnetism together with spin-glass behavior and pure spin-glass (or rather spin cluster glass) behavior (Figure 7).

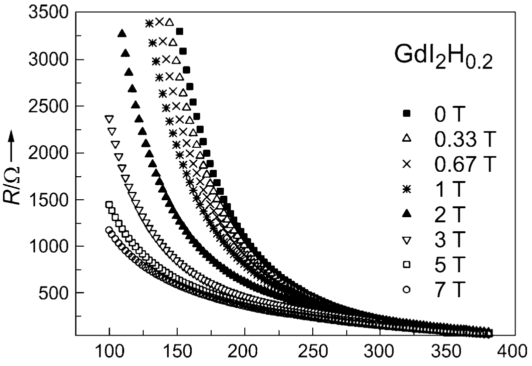

Figure 5. Electrical resistance of $GdI_2H_{0.2}$ as a function of external magnetic field.

The interpretation of the different phenomena follows from a visual picture presented in Figure 8.[15] In the planar net of Gd atoms, the H atoms take positions in the centers of the triangles. Once the H atom is in this position it changes the magnetic coupling between the surrounding Gd atoms from ferromagnetic to antiferromagnetic. In an Ising-type system antiferromagnetism is frustrated, because in a triangle an antiparallel alignment of all the magnetic moments is impossible. Frustration is also introduced into neighboring triangles which are not occupied by H atoms. At the chosen composition $GdI_2H_{0.25}$ percolation still exists, that is, pathways of ferromagnetically coupled Gd atoms allow electrons to move with no spin–flip barrier. At a critical filling of 1/3 of the available H sites, frustration covers all triangles. Further hydrogenation does not change the ratio of ferro- and antiferromagnetic interaction any more, but only removes conduction electrons through hydride formation until the salt-like insulator $Gd^{3+}I^{-}{}_2H^{-}$ is reached, which neatly explains both the magnetic as well as the electrical behavior. The sharp change in properties with filling of 1/3 of the H atom positions indicates an ordered array in each layer although scattering experiments do not show superstructures, because of lack of coherence between the layers.

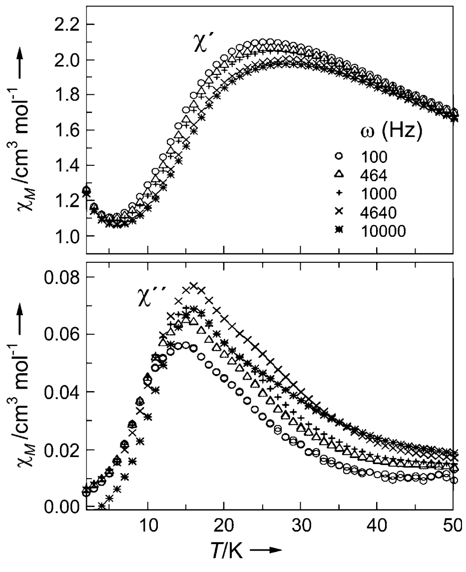

Figure 6. Real part (top) and imaginary part (bottom) of the magnetic susceptibility measured for $GdI_2H_{0.42}$ at different frequencies indicating spin-glass behavior.

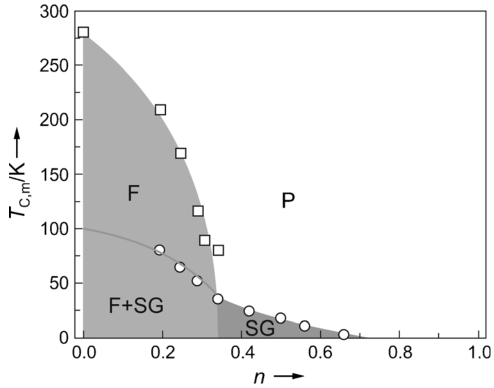

Figure 7. Magnetic phase diagram of GdI_2H_n comprising areas of paramagnetism, ferromagnetism characterized by T_c, and spin-glass behavior characterized by the melting temperature T_m.

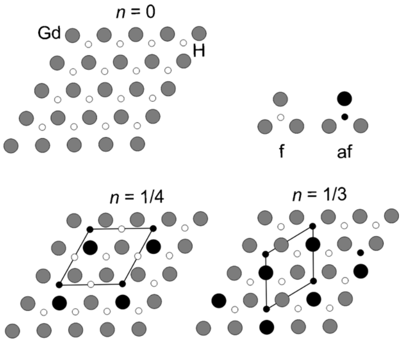

Figure 8. Top: Triangular layer of Gd atoms in the structure of GdI_2 with the possible positions for hydrogen atoms indicated as empty spheres, bottom: patterns of local ferro- and antiferromagnetic order in $GdI_2H_{0.25}$ and $GdI_2H_{0.33}$, occupied H positions drawn as filled spheres.

To summarize the results presented in this Section, hydrogen is absorbed by low-valence *RE* compounds which have excess electrons in *M*–*M* bonding states that can be transferred to the H atoms. What seems like a necessary and sufficient situation, however, may not be sufficient and not even necessary, as will be illustrated with the following exceptions.

3. No Reaction with Hydrogen in spite of Excess Metal Valence Electrons

There are exceptions to the rule mentioned above. The first to be analyzed concerns low-valence *RE* compounds which do not absorb hydrogen in spite of having a surplus of metal valence electrons. The reasons are many, based on special electronic bonding conditions or electrostatics or both. Gd_2Cl_3 is a good example to start with. Its crystal structure is composed of linear chains of edge-sharing Gd_6 octahedra encapsulated by Cl atoms.[16] In the ionic-limit bonding can be formulated as $Gd^{3+}{}_2Cl^-{}_3{\cdot}3\,e^-$. The $4f^7$ core of trivalent Gd is clearly demonstrated by the photoelectron spectrum which is characterized by a narrow f band with no multiplet splitting. The excess d electrons are involved in localized *M*–*M* bonds which lead to semiconducting behavior. The origin of electronic localization could be a Peierls distortion of the chain, however, it is rather the special condition of an avoided crossing of bands in the electronic band structure that leads to a closed-shell condition with stable *M*–*M* bonds and significantly lowered energy of the d bands.[17] The excess electrons are simply not available to be transferred to hydrogen.

A similar situation is met with LaI_2, which, like GdI_2, is metallic. Whereas it is difficult to prepare GdI_2 free of traces of hydrogen, LaI_2 is a truly binary compound entirely free of hydrogen. The different behavior has an electronic reason based on structure.[18] GdI_2 crystallizes with a triangular net of Gd atoms (as mentioned above) with electron-deficient 3-center bonds.[19] These are ideally suited to mix with the H1s orbital. In contrast, LaI_2 contains quadratic nets of La atoms in its structure, bonded by 2-center σ-bonds which offer no significant overlap with the H1s orbital. If LaI_2 is forced to absorb hydrogen, the quadratic net collapses into the close-packed triangular net resulting in intergrowth structures of the Nb and Mo dichalcogenide types, and these can then bind hydrogen. As indicated in Figure 9a there is a large miscibility gap between LaI_2 and the hydrogenated phase LaI_2H_n.[20]

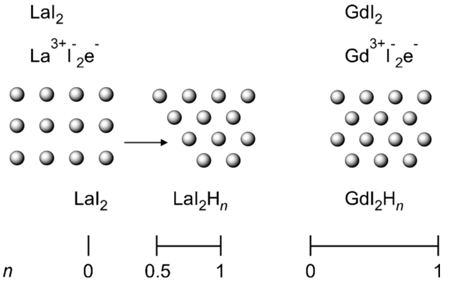

Figure 9. Comparison of the metal-atom nets in the structures of LaI_2 and GdI_2. Only the triangular nets are capable of incorporating hydrogen leading to a miscibility gap for LaI_2H_n and a complete range of homogeneity for GdI_2H_n.

The case of the monoiodide LaI is even more perplexing. The compound was discovered rather recently.[21] Its synthesis looked somewhat strange, because La metal and LaI_3 had to be heated in a sealed Ta capsule for months, traces of Zn seemed to help the reaction to proceed and yet the yield was low. Some suspicion about its binary structure arose based on our earlier experience with "monohalides" stabilized by hydrogen. However, using Na in the reduction reaction and choosing LaI_2 as starting material, LaI could be prepared in quantitative yield within a few days.[22] Clearly, the layered structure of LaI_2 allows a different pathway for the reaction than the three-dimensional network of LaI_3. Many careful checks for a possible contamination definitely excluded the presence of hydrogen. There is an interesting electronic and electrostatic reason why LaI stays as a pure binary in spite of the presence of two excess metal valence electrons. The crystal structure is of the NiAs type, however, with an exceptionally large *c*/*a* ratio representing rather a layered structure. The triangular layers of La atoms should be well suited for the incorporation of H atoms. The result of a calculation of the electron localization function (ELF), however, gives an explanation as to why hydrogen absorption does not occur (Figure 10). The attractor representing the three-center bond lies out of the plane of the La atoms, and the electrostatic origin of this deviation is clearly due to the repulsion by the iodide ion above the center of the triangle. Placing an H atom into this position would increase this repulsion still further and, hence, the hydrogen cannot be incorporated.[22]

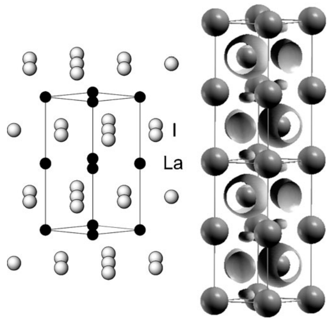

Figure 10. Layered crystal structure of LaI (left) and electron localization function (ELF) at an iso-value $\eta = 0.44$ (right) indicating a repulsive interaction between the electrons in the multicenter bonds of the La_3 triangle and the I^- ions.

4. Reaction with Hydrogen in spite of the Absence of Excess Metal Valence Electrons

The final example addresses the case of a *RE* compound, La_2C_3, which lacks low valence and can be described as a normal-valence compound with no excess metal valence electrons being present. Its cubic structure is formulated as an ethenide $La^{3+}{}_4(C_2{}^{4-})_3$ which becomes a metal "by accident" as a result of backbonding from the occupied $C_2\pi^*$ states into empty La d states, and the proximity of localization and delocalization may be the origin of superconductivity in La_2C_3.[23] This carbide presents many surprises, starting with its composition. As a result of a large number of investigations it was concluded that La_2C_3 exhibits a significant homogeneity range,[24] but prolonged annealing of samples within this range reveals that they split into stoichiometric La_2C_3 and a metal-rich phase $La_2C_{2.67}$, clearly identified by their respective sharp transitions to superconductivity, La_2C_3 becomes superconducting at 12 K and the metal-rich phase around 5 K, respectively.[25] Even more surprising is the reaction of La_2C_3 with hydrogen. At a moderate temperature of 450 K the compound starts to absorb hydrogen and becomes amorphous, as shown in X-ray and neutron diffraction patterns, but also even in electron diffraction, for which the scattering coherence length is much shorter. In the electron microscope the hydrogen is desorbed within seconds, and the diffraction pattern of La_2C_3 evolves.

The hydrogenation reaction is surprising for several reasons, first, that it proceeds at such mild conditions, second, that it proceeds with no excess of metal valence electrons being present and, last but not least, that an amorphous product results. Starting from stoichiometric La_2C_3 the product has the composition $La_2C_3H_{1.5}$. A first question concerns the bonding of hydrogen: Does the H atom bind to the C_2 unit or does it enter as discrete hydride anion? The strict stoichiometry of the phase indicates the hydride anion version to be true, and crystallographic data are in favor of hydride formation. In the structure of La_2C_3 the C_2 units reside in a bisdisphenoid coordination by La atoms, and the C–C distance of 130 pm corresponds to the anticipated ethenide ion with a slight shortening due to the backbonding effect mentioned above. In the space group $I\bar{4}3d$ the La atoms occupy Wyckoff position 16*c* and offer the bisdisphenoidal voids in 12*a* for the C_2 units together with distorted tetrahedral voids in 12*b*. So, the occupation of all the tetrahedral voids by H atoms results in the experimentally determined composition $La_4(C_2)_3H_3$. Indeed, inelastic neutron scattering experiments identified vibrations at 125 meV for H and 85 meV for D and corroborated the assumption that these atoms are discrete and occupy the tetrahedral voids.[26]

The necessity for electroneutrality leads to the roots of the amorphization process. It is interesting to note that hydrogen also acts as an oxidizing agent towards the anionic C_2 species in contrast to common conception, reminiscent of the change of the noble-metal platinum being oxidized from +2 to +4 in the reaction of K_2PtH_4 to K_2PtH_6.[27] To maintain electroneutrality in $La_2C_3H_{1.5}$ some of the C_2^{4-} ions have to be oxidized to C_2^{2-} ions resulting in a charge distribution of $La^{3+}{}_4(C_2C_2C_2)^{9-}H^-{}_3$. All the 12*a* positions are fully occupied by C_2 units in the stoichiometric compound, however, these C_2 units are not all the same, they are a mixture of C_2^{4-} and C_2^{2-} ions. The charge sum 9− can be realized in many different ways, for example, by occupying all the voids with a 50 %:50 % mix of C_2^{4-} and C_2^{2-} ions, but also, for example, with 50 %:50 % in one void, 40 % and 60 % in the other and 60 % and 40 % in the third. In this way a pronounced local disorder of the C_2 units originates which is transferred into a disorder of the sublattice of the heavy La atoms which dominate the scattering. This situation is characteristic of a so-called anti-glass.[28] In a normal glass, for example, silicate glass, the well defined building units of SiO_4 tetrahedra are connected with no long-range translational order. In an anti-glass the opposite is true. The long-range order is preserved but the shape and size of the building units, in this case the bisdisphenoid coordination polyhedra, vary statistically. It was Hosemann[29] who did extended research into what he called the "paracrystalline" state. $La_2C_3H_{1.5}$ is a good example for such a paracrystal.

In a dynamic vacuum at around 900 K hydrogen desorption from $La_2C_3H_{1.5}$ results in well-crystallized superconducting La_2C_3, similar to the result obtained in an electron microscope mentioned above. When the thermal treatment is performed at the same temperature in a hydrogen atmosphere of normal pressure,[25] CH_4 is slowly liberated, and finally a reaction product is formed which has the composition La_2CH_4 and exhibits a diffuse fcc-type X-ray pattern leading to lattice parameters which are different from those of LaH_2 by only 0.5 %. But in contrast to LaH_2, which forms LaH_3 upon cooling to room temperature in an atmosphere of hydrogen, La_2CH_4 stays as it is. The difference in behavior finds a simple explanation in terms of the crucial condition described in Section 2: The excess metal valence electron in $La^{3+}H^-{}_2{\cdot}e^-$ can be "titrated" by incorporating further hydrogen, but $2\,La_2CH_4 = La^{3+}{}_4C_2^{4-}H^-{}_8$ is an electronically saturated normal-valence compound which does not react with hydrogen. Last but not least, when the hydrogenation of La_2C_3 is performed at a temperature slightly above 1100 K in a closed Ta tube, introducing hydrogen by diffusion through the container wall and avoiding CH_4 to escape, yet another reaction is observed according to the relationship $2\,La_2C_3 + H_2 = 2\,LaC_2 + La_2C_2H_2$. The X-ray powder pattern after subtracting the LaC_2 component closely matches a structural model for a layered intergrowth of LaC_2 and LaH_2 (Figure 11) in which the ethenide ion of the educt is again preserved in an electron-precise compound.[25]

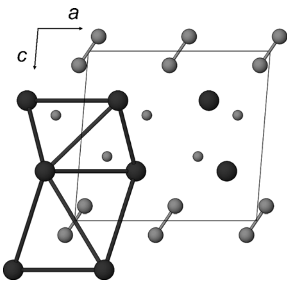

Figure 11. Structure model for $La_2C_2H_2$, atoms La, C, and H drawn with decreasing sizes.

5. Conclusion

Metal–metal bonding is a quite common phenomenon in the solid-state chemistry of low-valence compounds of the rare-earth metals, but one that is still waiting to be realized in their molecular compounds. The electrons involved in *M–M* bonding play an important role in the reaction with hydrogen. With low-valence *RE* compounds an electron transfer to the hydrogen atom is frequently found, and the hydrogen is reduced to the hydride anion. Repulsive interactions between all the anions are evidenced by specific structural changes. Hydrogen absorption can be blocked in spite of the presence of excess metal valence electrons owing to these electrostatic and/or special electronic conditions. As a rare exception hydrogen absorption occurs with the necessary electrons being provided by redox labile anions in the lattice. The interplay of d electrons in bands with *M*–*M* bonding character, 4f core-state electrons, and hydride anions is reflected in unusual electric and magnetic properties.

Received: December 5, 2011

---

[1] *Gmelin Handbuch der Anorganischen Chemie*, *C1*, Springer, Berlin, **1974**, pp. 1–85.
[2] P. Vajda, *Handbook on the Physics and Chemistry of Rare Earths*, vol. 20 (Eds.: K. A. Gschneidner, Jr., L. Eyring), North Holland, Amsterdam, **1995**, pp. 207–291.
[3] T. J. Udovic, J. J. Rush, Q. Huang, I. S. Anderson, *J. Alloys Compd.* **1997**, *253–254*, 241–247.
[4] A. Simon, H. Mattausch, H. Holzer, *Angew. Chem.* **1976**, *88*, 685–686; *Angew. Chem. Int. Ed. Engl.* **1976**, *15*, 624–625.
[5] R. K. Poeppelmeier, J. D. Corbett, *Inorg. Chem.* **1977**, *16*, 294–297.
[6] A. Simon, H. Mattausch, R. Eger, *Z. Anorg. Allg. Chem.* **1987**, *550*, 50–56.
[7] A. Simon, *Z. Anorg. Allg. Chem.* **1967**, *355*, 311–322.
[8] F. Dübler, H. Müller, C. Opitz, *Chem. Phys. Lett.* **1982**, *88*, 467–472.
[9] C. Bauhofer, H. Mattausch, G. J. Miller, W. Bauhofer, R. K. Kremer, A. Simon, *J. Less-Common Met.* **1990**, *167*, 65–79.
[10] M. Ruck, A. Simon, *Z. Anorg. Allg. Chem.* **1992**, *617*, 7–18.
[11] A. Simon, H. Mattausch, G. J. Miller, W. Bauhofer, R. K. Kremer, *Handbook on the Physics and Chemistry of Rare Earths*, vol. 15 (Eds.: K. A. Gschneidner, Jr., L. Eyring), North Holland, Amsterdam, **1991**, pp. 191–285.
[12] J. E. Mee, J. D. Corbett, *Inorg. Chem.* **1965**, *4*, 88–93.
[13] C. Felser, K. Ahn, R. K. Kremer, R. Seshadri, A. Simon, *J. Solid State Chem.* **1999**, *147*, 19–25.
[14] M. Ryazanov, A. Simon, R. K. Kremer, H. Mattausch, *J. Solid State Chem.* **2005**, *178*, 2339–2345.
[15] A. Simon, H. Mattausch, M. Ryazanov, R. K. Kremer, *Z. Anorg. Allg. Chem.* **2006**, *632*, 919–929.
[16] D. A. Lokken, J. D. Corbett, *Inorg. Chem.* **1973**, *12*, 556–559.
[17] D. W. Bullett, *Inorg. Chem.* **1985**, *24*, 3319–3323.
[18] O. Jepsen, O. K. Andersen, *Z. Phys. B* **1995**, *97*, 35–47.
[19] Y. Tian, T. Hughbanks, *Inorg. Chem.* **1993**, *32*, 400–405.
[20] M. Ryazanov, A. Simon, H. Mattausch, *Z. Anorg. Allg. Chem.* **2004**, *630*, 104–108.
[21] J. D. Martin, J. D. Corbett, *Angew. Chem.* **1995**, *107*, 234–236; *Angew. Chem. Int. Ed. Engl.* **1995**, *34*, 233–235.
[22] M. Ryazanov, L. Kienle, A. Simon, H. Mattausch, *Inorg. Chem.* **2006**, *45*, 2068–2073.
[23] A. Simon, *Angew. Chem.* **1997**, *109*, 1873–1891; *Angew. Chem. Int. Ed. Engl.* **1997**, *36*, 1788–1806.
[24] K. A. Gschneidner, F. W. Calderwood, *Bull. Alloy Phase Diagr.* **1986**, *7*, 421–436.
[25] A. Simon, T. Gulden, *Z. Anorg. Allg. Chem.* **2004**, *630*, 2191–2198.
[26] G. Auffermann, A. Simon, T. Gulden, G. J. Kearly, A. Ivanov, *Z. Anorg. Allg. Chem.* **2001**, *627*, 307–311.
[27] W. Bronger, G. Auffermann, P. Mueller, *J. Less-Common Met.* **1986**, *116*, 9–15.
[28] M. Trömel, *Z. Kristallogr.* **1988**, *183*, 15–26.
[29] R. Hosemann, F. J. Balta-Calleja, *Ber. Bunsenges. Phys. Chem.* **1980**, *84*, 91–95.